frontiers | Frontiers in Mechanical Engineering

TYPE Original Research
PUBLISHED 30 August 2022
DOI 10.3389/fmech.2022.978714

OPEN ACCESS

EDITED BY
Zhigang Dong,
Dalian University of Technology, China

REVIEWED BY
Chongjun Wu,
Donghua University, China
Guijian Xiao,
Chongqing University, China

*CORRESPONDENCE
Xinjiang Liao,
xinjiang@hqu.edu.cn

SPECIALTY SECTION
This article was submitted to Digital Manufacturing,
a section of the journal
Frontiers in Mechanical Engineering

RECEIVED 26 June 2022
ACCEPTED 21 July 2022
PUBLISHED 30 August 2022

CITATION
Yang Z, Huang H and Liao X (2022), Influence of cutting parameters on wear of diamond wire during multi-wire rocking sawing with reciprocating motion.
Front. Mech. Eng 8:978714.
doi: 10.3389/fmech.2022.978714

Influence of cutting parameters on wear of diamond wire during multi-wire rocking sawing with reciprocating motion

Zixing Yang[1,2], Hui Huang[1,2,3] and Xinjiang Liao[2,3]*

[1]Institute of Manufacturing Engineering, Huaqiao University, Xiamen, China, [2]Collaborative Innovation Center of Advanced Manufacturing Technology and Equipment for Stone Industry, Xiamen, China, [3]College of Mechanical Engineering and Automation, Huaqiao University, Xiamen, China

Multi-wire cutting with diamond wire saw has gradually become the main processing method for hard-and-brittle materials due to its small kerf loss and high machining accuracy. However, the diamond wire saw will inevitably suffer wear during the process of machining, and hence affects the quality of the cut surface. In this paper, a wire saw wear model was established, and the wear at different positions on the wire saw was theoretically calculated by correlating the volume of the workpiece removed by the unit wire saw to the wire saw wear. The iteration method was used to calculate the wear of the wire saw after cutting by superimposing the wear caused by every monolithic wafer. Based on this wear year model of the wire saw, the influence of multi-wire cutting parameters and the shapes of the workpiece on the wire saw wear was discussed through numerical simulation. The simulation results showed that the feed speed of the workpiece and the length of the wire saw had an obvious effect on the maximum wear of the wire saw, and the maximum rocking angle, wire speed, and reciprocating times had little effect on the maximum wear of the wire saw. The wear curve of the circular workpiece wire saw is unstable in the whole process, and the wear curve of the rectangular workpiece wire saw changes at the beginning and end, and the middle is stable.

KEYWORDS

multi-wire cutting, wire saw, wear, cutting parameters, numerical simulation

1 Introduction

Wafer slicing is an essential step in the fabricating of electronic device chips, which transforms crystalline materials from sticks to flakes. Multi-wire sawing with diamond wire saw is the main technology used in the semiconductor industry for slicing sapphire (Kim et al., 2013, 2015; Lee et al., 2016), silicon carbide (Maeda et al., 2014; Huang et al., 2016; Wang et al., 2017; Zhao et al., 2021) and silicon ingots (Chen et al., 2019; Sekhar et al., 2020). However, during the multi-wire sawing process, the diamond wire saw would inevitably wear out (Kumar et al., 2016; Knoblauch et al., 2018; Yin et al., 2021).

The wear of a diamond wire saw during the cutting process led to an increase in both cutting and normal forces (Pala et al., 2018). Moreover, the wear changed the surface characteristics of the diamond wire saw and influenced the cutting performance along the

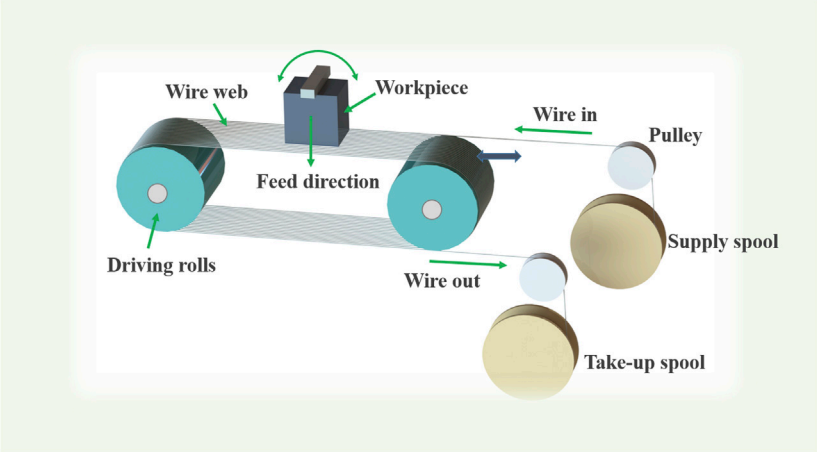

FIGURE 1
The schematic of multi-wire saw cutting.

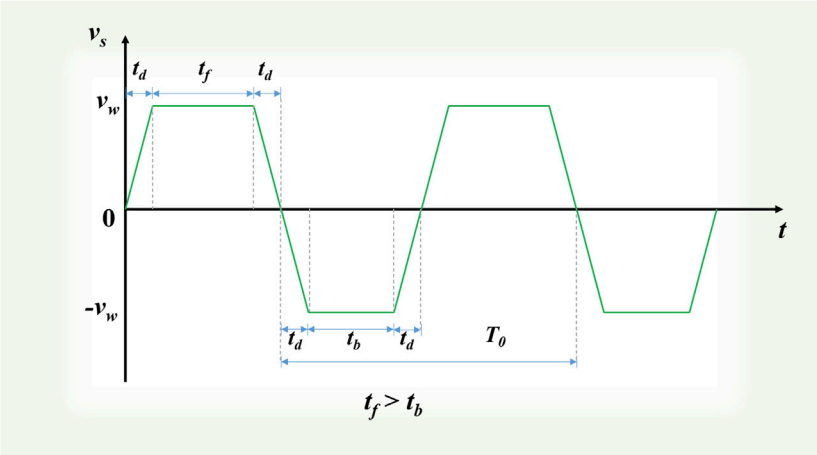

FIGURE 2
The wire saw speed changing with time during the multi-wire saw cutting.

ingot location (Kim et al., 2013). Exploring the wear mechanism of diamond wire saw during slicing is of importance to improve the surface quality of the wafer and becomes a research hotspot issue. The wear forms and the surface characteristics of diamond wire saw in single-wire cutting were usually studied by a scanning electron microscope (Gao et al., 2016; Kumar et al., 2016; Liu and Zhu, 2022). The diamond wire saw would experience initial wear, stable wear, and severe wear (Yin et al., 2021). To quantify the wear of diamond wire saw, the wire saw diameter, grit protrusion height, and grit volume was selected as an index to study the wear (Li et al., 2015; Pala et al., 2018; Liu and Zhu, 2022). However, only interval sampling, observation, and wear characterization of the experimental results are carried out for the single-wire cutting process. In the multi-wire cutting process, considering that the diamond wire saw from entering the processing area to exiting the processing area involves the machining of hundreds of wafers, more serious wear of the wire saw would suffer than that of the single-wire cutting process. The wear of the diamond wire saw in the multi-wire cutting process is more complex and difficult to directly observe the wear characteristics for the whole diamond wire saw used. To reveal the wear law of diamond wire saw during the multi-wire cutting process is significant to understanding the formation of the cut quality of wafers. However, little literature was studied on the wear of diamond wire saws for the multi-wire cutting process.

This paper reports the theoretical analysis of the wire saw wear during the multi-wire cutting process with rocking and reciprocating motions. The effects of maximum rocking angle, wire speed, workpiece feed speed, reciprocating times, setting out the length of wire saw, and the workpiece shape on the wear of wire saw were studied.

2 Establishment of wire saw wear model

2.1 Assumptions of the wire saw wear model for multi-wire saw process

Figure 1 illustrates the schematic diagram of multi-wire cutting processing, which includes the reciprocating motion of the diamond wire saw, and the downward feeding and rocking motions of the workpiece. The diamond wire saw forms a wire web through a specific winding method. The distance that a wire saw moves from the middle of a wafer to the middle of an adjacent wafer is Sp.

Illustrates the change in wire speed during the reciprocating motion of the wire saw. The formulas in Eq. 1 describe the movement of the diamond wire saw in each stage shown in Figure 2.

$$\begin{cases} T = \dfrac{60}{f} \\ t_f + t_b + 4 \times t_d = T \\ l = \dfrac{L}{f} \\ t_d = \dfrac{v_w}{a} \\ t_f + t_b = T - 4 \times t_d \\ t_f - t_b = \dfrac{l}{v_w} \end{cases} \tag{1}$$

where v_s: wire saw speed, v_w: maximum wire speed, a: accelerated speed of diamond wire saw (measured as 4 m/s^2), L: setting out length per minute, l: setting out length per cycle; f: reciprocating times per minute, t_f: the time that the wire saw uniform moves forward in one reciprocating cycle, t_b: the time that the wire saw uniform moves backward in one reciprocating cycle, t_d: the time that the wire speed accelerates to the highest speed or decelerates to zero, T_0: the time for one reciprocation of the wire saw. In one cycle of the multi-wire reciprocating diamond, wire saw, the wire feeding time is ($2t_d + t_f$). After completion, it will make a loop movement, and the loop time is ($2t_d + t_b$).

$$\begin{cases} x_1 = v_w t_f + v_w t_d \\ x_2 = v_w t_b + v_w t_d \end{cases} \tag{2}$$

where x_1: incoming wire saw length in one cycle, x_2: loop length in one cycle of the wire saw. Therefore, at the end of one cycle, the length of the used wire saw taken up by the take-up spool is v_w (t_f - t_b), which is also the length of the new wire saw entering the processing area in the next cycle. In the theoretical analysis of wire saw wear, the following assumptions were proposed: ① Assuming that the abrasive particles are evenly distributed on the wire saw, the number of abrasive particles per unit length on the wire saw is the same; ② Assuming that the line starts to enter the processing area, the coordinate system of the line is established. From the position where the workpiece starts to enter the processing, the corresponding coordinate system is also established; ③ Assuming that the diameter of the wire saw is a certain value during the processing, the wire saw has no length deformation, and there is no wire bow during the cutting process; ④ The influence of speed fluctuations on the wear of the wire saw during the acceleration and deceleration process is not considered; ⑤ In the reciprocating process of the wire saw, the removal volume of the workpiece corresponding to each reciprocating cycle is analyzed. Meanwhile, according to the reference (Li et al., 2015), the wear of the wire saw is related to the area processed by the wire saw, which could be described as S by Eq. 3:

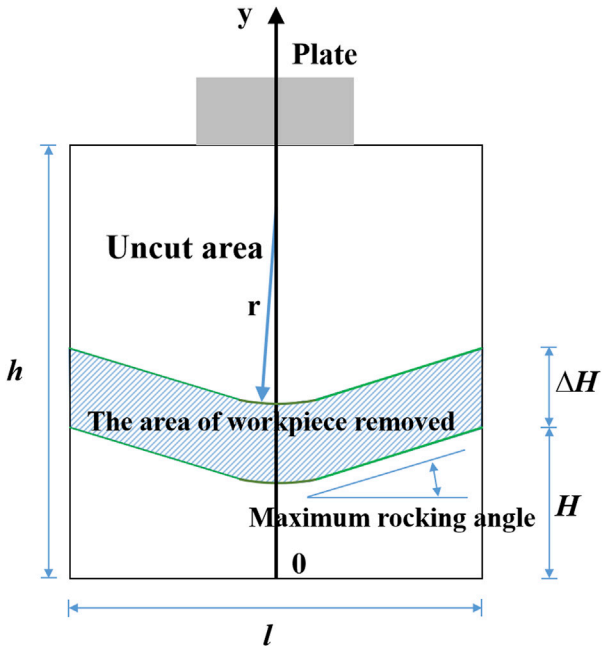

FIGURE 3
Wire saw area chart for a certain period of the rectangular wafer.

$$S = p \times \mathrm{k} \tag{3}$$

where S: the wear degree of the wire saw, p: the volume of the workpiece removed by the wire saw, k: a coefficient reflects the cutting ability of the wire saw, which varies slightly with wear and could be regarded as a constant.

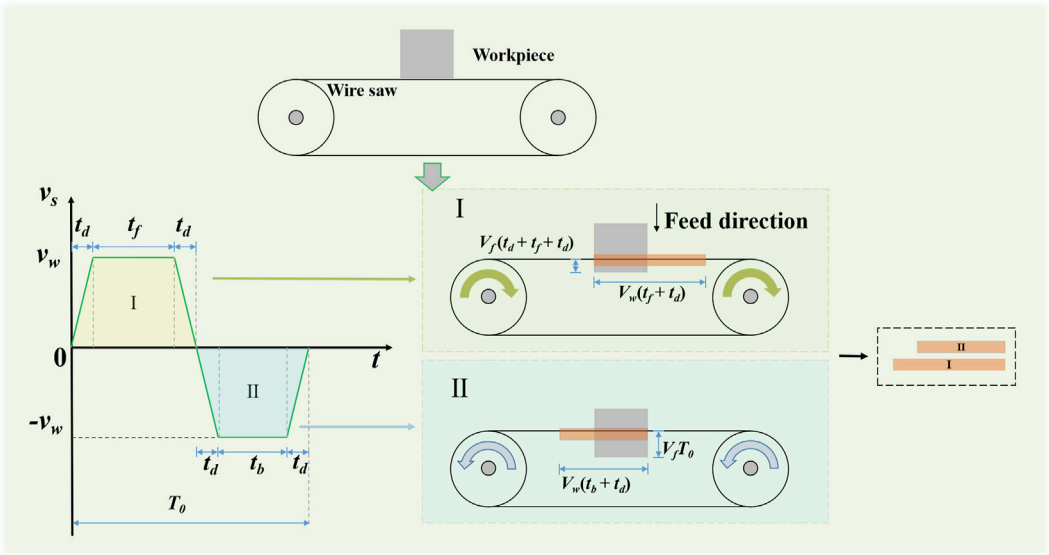

FIGURE 4
Wire movement and wear distribution of wire saw in one reciprocating cycle.

2.2 Wire saw wear model for cutting one rectangular wafer

The area of the workpiece cut by the wire saw per cycle is equal to the area formed by the wire saw track between cycles. The wire saw trajectory can be mainly seen as three segments, which are straight line, arc line, and the straight line (Huang et al., 2016). When the wire saw trajectory was simplified, it can be considered that it consists of three parts, namely, a straight line with symmetrical ends at both ends, and an arc tangent to the straight line. The central angle corresponding to the arc is equal to twice the maximum rocking angle. It is considered that during the reciprocating feeding process of the wire saw, the wire saw trajectories are parallel along the feeding direction.

For the regular shape of the rectangular workpiece, the volume removal per cycle is relatively consistent during the cutting process. Figure 3 illustrates the components of each movement in multi-wire cutting, which are the rocking movement of the workpiece, the feeding movement of the workpiece, and the reciprocating movement of the wire saw. At the same time, it also points out the stable stage of sawing area in one cycle in the process of rectangular workpiece processing. In Figure 3, $\boldsymbol{r}$ is the rocking radius of the workpiece during the rocking process; $\boldsymbol{H}$ is the height of the workpiece relative to the wire saw that the workpiece has been fed by the end of the last reciprocating cycle; $\Delta\boldsymbol{H}$ is the height of the workpiece feeding in the next cycle. $\boldsymbol{H}$ is the height of the rectangular workpiece, and $\boldsymbol{l}$ is the width of the rectangular workpiece, as shown in Figure 3.

The value of $\boldsymbol{p_{cycle}}$ is based on the simplification of the trajectory in the figure shown previously, which is the area formed by the periodic trajectory and the previous periodic trajectory multiplied by the width of the wire saw, that is, the volume is removed.

Figure 4 illustrates a reciprocating cycle of the wire saw is generally divided into two stages (I and II), namely the wire saw inlet stage and the outlet stage. In the first stage, the workpiece is fed down a distance $v_w\ (t_f + t_d)$. At the end of the second stage, that is, after one cycle, the total downward feed distance of the workpiece is v_wT_0. The length of the wire saw corresponding to each stage and the volume of the workpiece will be processed in these two stages. Each cycle as a time interval can be used to calculate the volume of the workpiece removed by the wire saw in that cycle. The amount of workpiece volume removed by the wire saw in that cycle is divided by the sum of the reciprocating lengths of the wires involved in machining in that cycle. The removal volume of the workpiece per unit length of the wire saw in this cycle can be obtained.

In Figure 5, each color represents the movement of the wire saw in one cycle, and the length of different line segments in the length direction of the wire saw represents the corresponding reciprocating stage when the wire saw reciprocates. The longer one is the incoming line and the shorter one is the return line. The height of each rectangular grid represents the area of workpiece removal in one cycle. In the process of cutting a single wafer, the total wear amount corresponding to each wire saw position is equal to the sum of the heights of all rectangular lattices at their corresponding position, that is, at this position, the wires at all stages of the wire saw processing involved. Wire saw wear is superimposed on the length of the wire. Then, a wire saw wear model for wire sawing a single wafer is obtained.

Divide the wear amount of the wire saw in this cycle by the length of the wire saw movement in this section, and express the wear amount of the wire saw per unit length of the line as Eq. 4.

$$\left[q_{cycle,i}\right] = \left[p_{cycle,i}\right] \times \frac{d}{\left(t_f + t_b + 2 \times t_d\right) \times v_w} \tag{4}$$

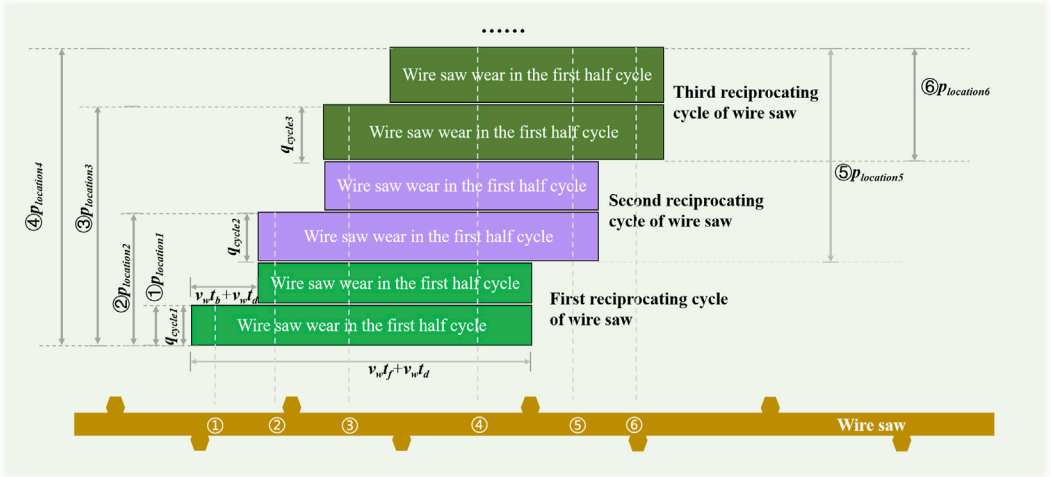

FIGURE 5
Wire movement and wear distribution of wire saw in multiple reciprocating cycles.

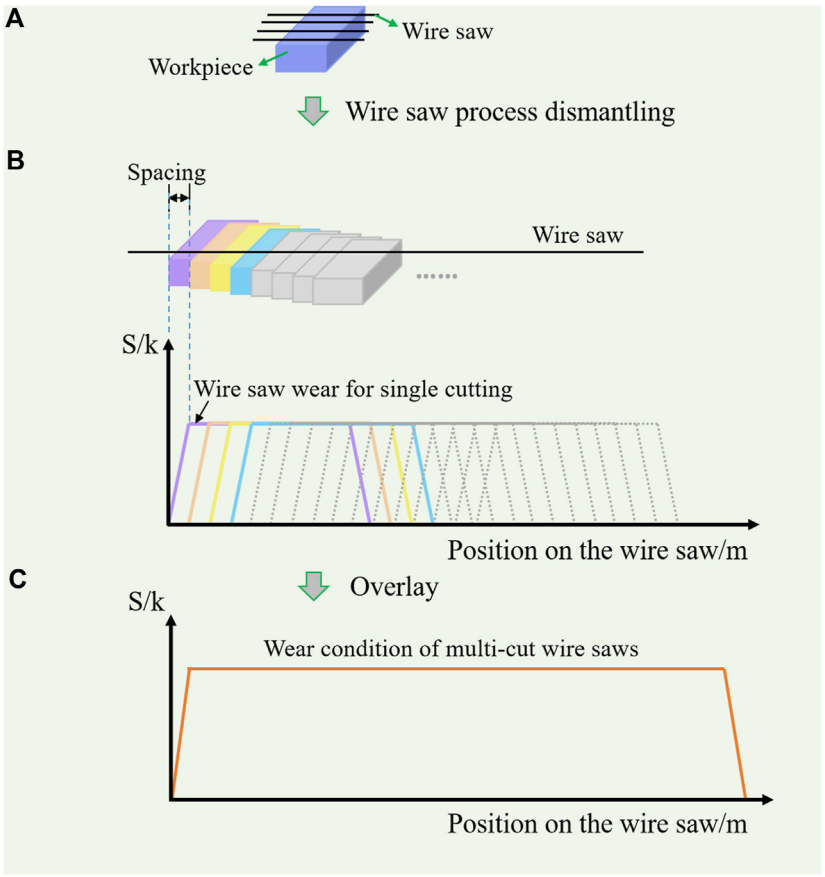

FIGURE 6
Wire saw wear overlay from single wafer to multi-wafer. **(A)** Schematic diagram of multi-wire sawing, **(B)** Unroll the wire saw of the wire web to achieve the wear on the wire saw for cutting each wafer, **(C)** Overlay the wear on the wire saw generated by each wafer.

where, $\boldsymbol{p_{cycle}}$: the area of workpiece removal in one cycle, $\boldsymbol{d}$: the diameter of the wire saw, $\boldsymbol{q_{cycle}}$: the workpiece removal volume corresponding to the wire saw per unit length in one cycle, $\boldsymbol{i}$: represents the number of complete reciprocating cycles experienced during sawing.

When using the matrix to calculate the wear amount of the wire, the wire needs to be discretized, the unit wear amount in the interval length is represented by numbers, and the digital interval represents the accuracy of the wire saw wear in the length direction.

The two wear conditions of the wire saw in one cycle are considered to be the same in height. Because without considering the wear of the wire saw, the reason why the height of the wire saw changes in this section of the wire is mainly affected by the parameters, as Eq. 5, but in a cycle, the parameters are unchanged, so in a cycle, the height of the wire saw is also will not change.

$$\begin{bmatrix}0\\0\\0\\0\\0\\0\\\vdots\\0\\0\\0\\0\\0\\0\end{bmatrix}+\begin{bmatrix}q_{cycle1}\\\vdots\\\vdots\\\vdots\\q_{cycle1}\\0\\\vdots\\0\\0\\0\\0\\0\\0\end{bmatrix}+\begin{bmatrix}0\\\vdots\\0\\q_{cycle1}\\\vdots\\q_{cycle1}\\0\\\vdots\\0\\0\\0\\0\\0\\0\end{bmatrix}+\begin{bmatrix}0\\\vdots\\0\\q_{cycle2}\\\vdots\\\vdots\\\vdots\\q_{cycle2}\\0\\\vdots\\0\\0\\0\\0\end{bmatrix}+\begin{bmatrix}0\\0\\0\\0\\0\\q_{cycle2}\\\vdots\\q_{cycle2}\\0\\\vdots\\0\\0\\0\\0\end{bmatrix}+\begin{bmatrix}0\\0\\0\\0\\0\\0\\q_{cycle3}\\\vdots\\\vdots\\\vdots\\q_{cycle3}\\0\\\vdots\\0\end{bmatrix}+\begin{bmatrix}0\\0\\0\\0\\0\\0\\0\\\vdots\\0\\q_{cycle3}\\\vdots\\q_{cycle3}\\0\\\vdots\\0\end{bmatrix}+\mathrm{L}$$

$$+\begin{bmatrix}0\\0\\0\\0\\0\\0\\0\\0\\q_{cycle,i}\\\vdots\\\vdots\\\vdots\\\vdots\\q_{cycle,i}\end{bmatrix}+\begin{bmatrix}0\\0\\0\\0\\0\\0\\0\\0\\0\\\vdots\\0\\q_{cycle,i}\\\vdots\\q_{cycle,i}\end{bmatrix}=\begin{bmatrix}p_{location,1}\\p_{location,2}\\p_{location,3}\\\vdots\\\vdots\\\vdots\\\vdots\\\vdots\\\vdots\\\vdots\\\vdots\\\vdots\\\vdots\\\vdots\\p_{location,n}\end{bmatrix}\tag{5}$$

According to the expression in Figure 5, calculate Eq. 5, where, $\boldsymbol{n}$: represents the number of elements used to represent the length of the wire saw calculated by the model after discretizing the length of the wire saw, $\boldsymbol{q_{cycle}}$ is summed to obtain the workpiece removal volume $\boldsymbol{p_{location}}$ per unit length corresponding to each position on the wire saw. $\boldsymbol{S_{location}}$ indicates the wear of the wire saw at this location. Eq. 6 is obtained from Eq. 3. It shows the relationship between $\boldsymbol{p_{location}}$ and $\boldsymbol{S_{location}}$ in the length direction of the discrete wire saw.

$$\begin{cases}p_{location}\times \mathrm{k}=S_{location}\\\begin{bmatrix}p_{location,1}\\p_{location,2}\\\vdots\\p_{location,n}\end{bmatrix}\times \mathrm{k}=\begin{bmatrix}S_{location,1}\\S_{location,2}\\\vdots\\S_{location,n}\end{bmatrix}\end{cases}\tag{6}$$

2.3 Wire saw wear model for cutting multiple rectangular wafers

Figures 6A, B illustrate that expanding the multi-wire cutting process and can be regarded as the same wire saw, cutting ingots at different intervals at the same time. The interval is related to the machine parameters. Overlay the wire saw wear in Figure 6B together to get the result in Figure 6C.

$$\begin{bmatrix}S_{location,1}\\\vdots\\S_{location,n}\\0\\\vdots\\0\\0\\0\\0\end{bmatrix}+\begin{bmatrix}0\\\vdots\\0\\S_{location,1+b}\\\vdots\\S_{location,n+b}\\0\\\vdots\\0\\0\end{bmatrix}+\begin{bmatrix}0\\\vdots\\\vdots\\0\\S_{location,1+2\times b}\\\vdots\\S_{location,n+2\times b}\\0\\\vdots\\0\end{bmatrix}+\cdots$$

$$+\begin{bmatrix}0\\0\\0\\0\\0\\\vdots\\0\\S_{location,1+(100-1)\times b}\\\vdots\\S_{location,n+(100-1)\times b}\end{bmatrix}=\begin{bmatrix}multiS_{location,1}\\multiS_{location,2}\\\vdots\\\vdots\\\vdots\\\vdots\\\vdots\\\vdots\\\vdots\\\vdots\\multiS_{location,n+(100-1)\times b}\end{bmatrix}\tag{7}$$

Therefore, in order to obtain the wire saw wear model of multi-wire cutting, the offset of the wire saw length is superimposed and the wire saw wear on the model of the wire saw cutting a single wafer is obtained.

2.4 Wire saw wear model for circular workpieces

The wire saw wear model for rectangular workpieces helps establish the wire saw wear model for circular workpieces. For round workpieces like Figure 7, the size of the wire saw feed direction is irregular, so the workpiece removal volume per cycle is different.

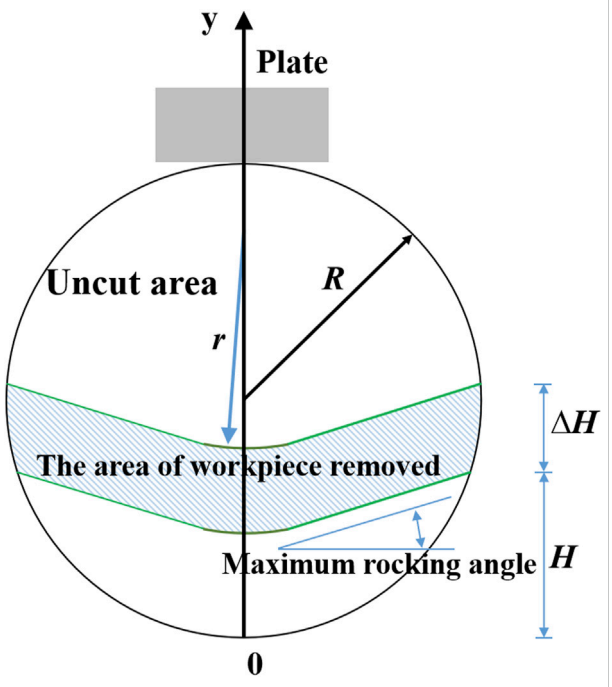

FIGURE 7
Wire saw area chart for a certain period of the circular wafer.

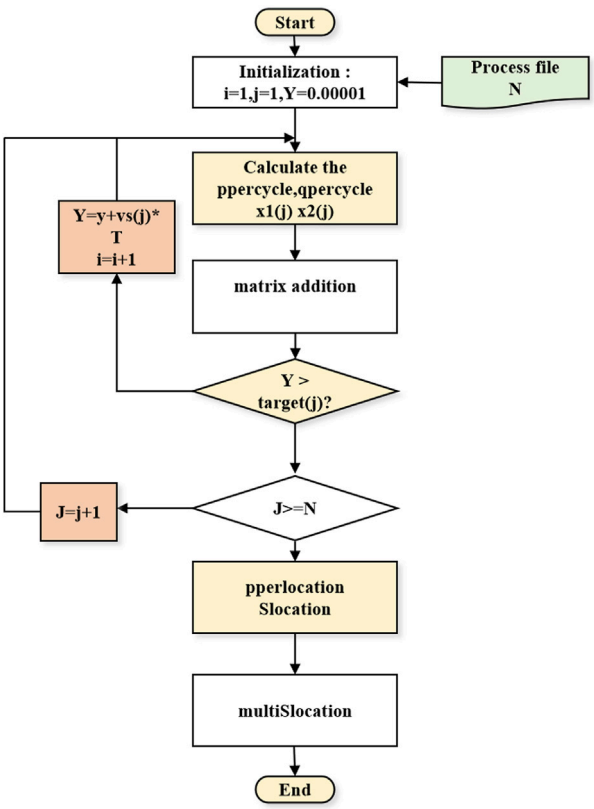

FIGURE 8
Numerical simulation flowchart of the wire saw wear model.

TABLE 1 Simulation process parameters.

Process parameters	Numerical value
Maximum rocking angle θ/°	2, 4, 6, 8, 10
Maximum wire speed v_w/m·s^{-1}	10, 15, 20, 25, 30
Workpiece feed speed v_f/m·min^{-1}	0.1, 0.15, 0.2, 0.25, 0.3
Setting out length per minute L/m·min^{-1}	8, 12, 16, 20, 24
Reciprocating times per minute f/minute^{-1}	0 0.4, 0.6, 0.8, 1.0, 1.2

3 Simulation parameters and steps

Table 1 is the parameter table used for numerical simulation. In the single-factor numerical simulation experiments, the selection is made according to the data in the table, only the value of one parameter is changed, and the values of other parameters remain unchanged. Table 2 shows the parameters of the two kinds of workpieces used for numerical simulation, and the rectangular workpiece and the circular workpiece are selected respectively. The workpiece size is the cross-sectional shape size of the two selected workpieces. R is the cross-sectional radius of the circular workpiece, as shown in Figure 7. Both h and R are related to the final cutting position of the workpieces.

TABLE 2 Simulation workpiece parameters.

	Rectangular workpiece	Round workpiece
Workpiece size	h = 0.2 m, l = 0.2 m	R = 0.1 m
Swing radius	0.3 m	0.2 m
Number of cut pieces	100	100
Sp	2 m	2 m

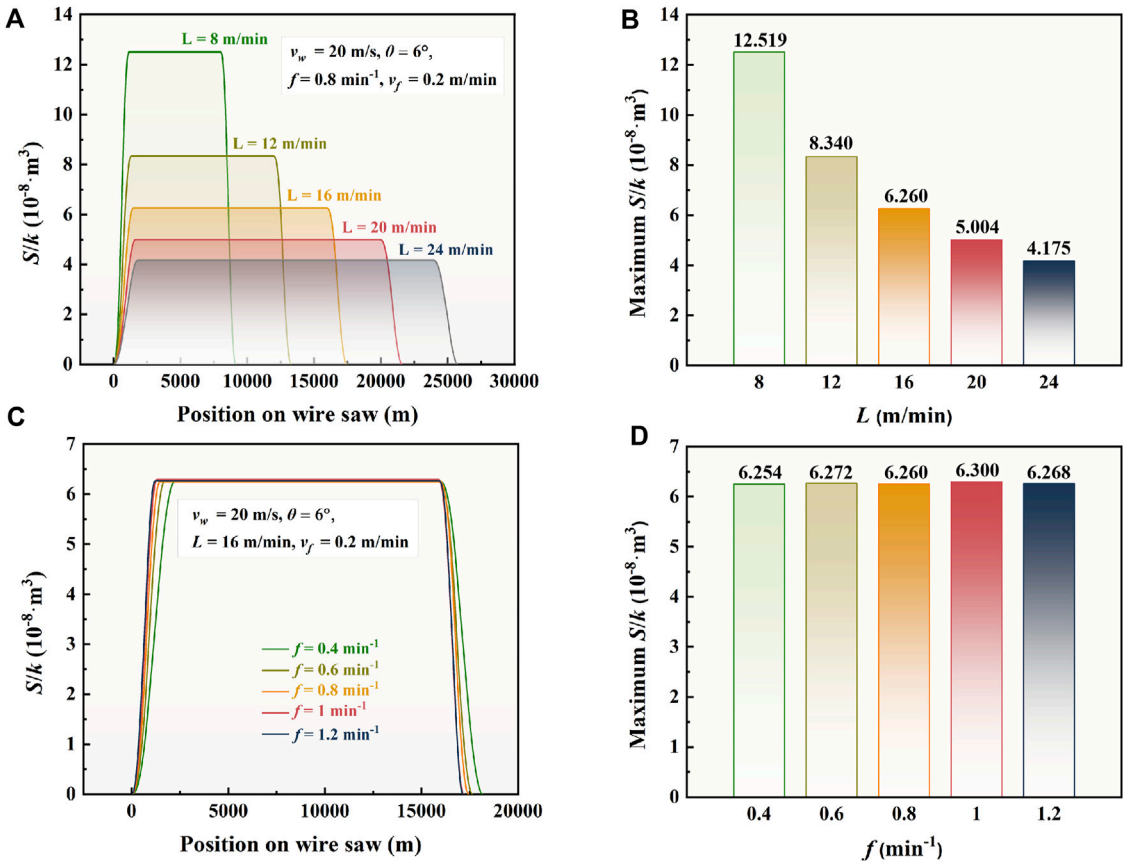

FIGURE 9
Variation of the wear amount of the wire saw on the rectangular workpiece and reciprocating frequencies. **(A,B)** illustrate the change in the setting out length will have an impact on the time difference between the take-up and pay-out. Under the condition that the wire feed length and speed remain unchanged, it directly affects the wire feed interval between two cycles, which in turn affects the number of superimpositions, thereby affecting the wear of the wire saw. **(C,D)** illustrate when the number of reciprocations changes, the time of the cycle will change, which will affect the time parameter of Eq. (1). The increase of t_b and t_f makes the value tend to decrease. At the same time, the difference between tb and t_f will affect the wire feeding length of each cycle feeding stage, by increasing the wire feeding length and then increasing the number of superpositions, the influence of the number of reciprocations on the wear of the wire saw remains roughly unchanged.

Considering the calculation time and calculation accuracy of the model, the accuracy of the model length is selected as 0.1 m. That is, the interval between matrix elements represents a length of 0.1 m.

The flowchart of the numerical simulation is shown in Figure 8. According to Figure 8, the steps of the numerical simulation are described as follows:

Step 1: Initialize the model, let $I = 1$, $j = 1$, and the cutting position $y = 0.000001$. Input the process file, extract the number of steps N, the ***target*** position target in each step, the maximum wire speed v_w, the number of reciprocations f, the feed speed v_f, the payout amount L, and the angle θ from the process file. j represents the number of steps in the current step, i represents the total number of cycles currently experienced, and y represents the processing position reached by the current wire saw.

Step 2: According to Eqs 1,2 and the simulation parameters of this step, calculate T, t_f, t_d, t_b, l, $x1(j)$, $x2(j)$. According to Section 2.2, calculate p_{cycle} and q_{cycle}.

Step 3: After calculating p_{cycle} and q_{cycle} in each cycle, according to the formulas in Section 2.2, the wear of each cycle is superimposed on the wire saw.

Step 4: Judgment $y >$ ***target***, if the condition is not established, proceed to the next cycle of processing, calculate the p_{cycle} of the cycle, and perform matrix superposition according to Section 2.2.

If the condition is established, it means that the wire saw has exceeded the processing area and should be stopped. At this time, it is necessary to use $j \geq N$ to judge whether there is the next process. If the condition of $j \geq N$ does not hold, there is the next process, the processing of the next process should be carried out, and the parameters corresponding to the next process are

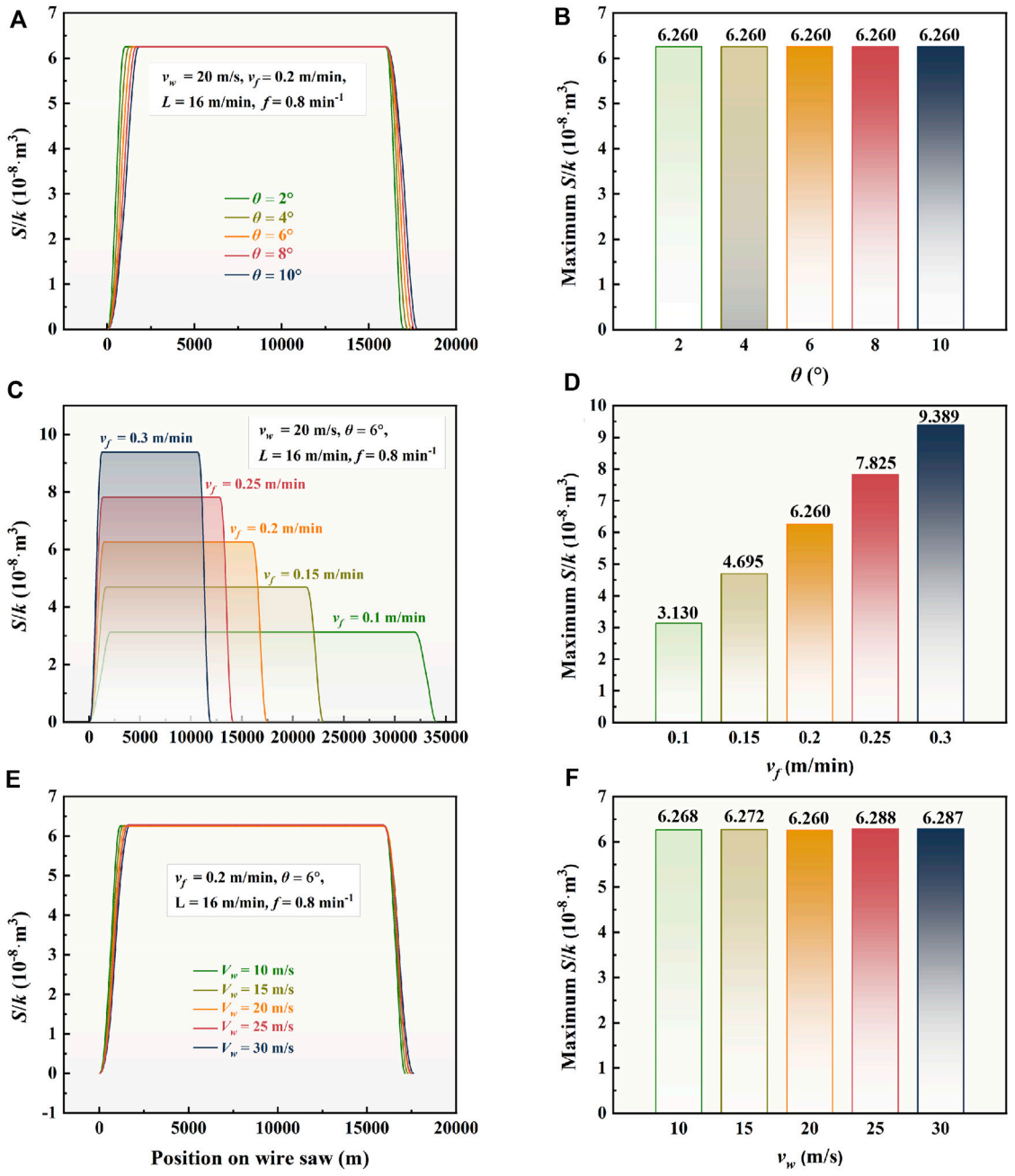

FIGURE 10
Variation of the wear amount of the wire saw on the rectangular workpiece under different maximum rocking angles, workpiece feed speeds and maximum wire speeds. Figure **(A,B)** illustrate the effect of the rocking angle on the maximum wear of the wire saw is not obvious, because the change of the angle is not obvious to the change of the sawing area in each cycle. Figure **(C,D)** illustrate the change of the workpiece feed speed has obvious changes to the maximum wear amount of the wire saw. This is because the change in the workpiece feed speed will cause the sawing area to follow the change in each cycle. Figure **(E,F)** illustrate the change of the wire speed has no obvious effect on the maximum wear amount of the wire saw.

substituted into Step 2. For calculation. If the $\boldsymbol{j \geq N}$ condition is established, it means that there is no next process, and the processing should be quit.

Step 5: After superimposing the wire saw wear of all cycles calculate the wire saw wear $\boldsymbol{S_{location}}$ and $\boldsymbol{p_{location}}$ for cutting a single wafer.

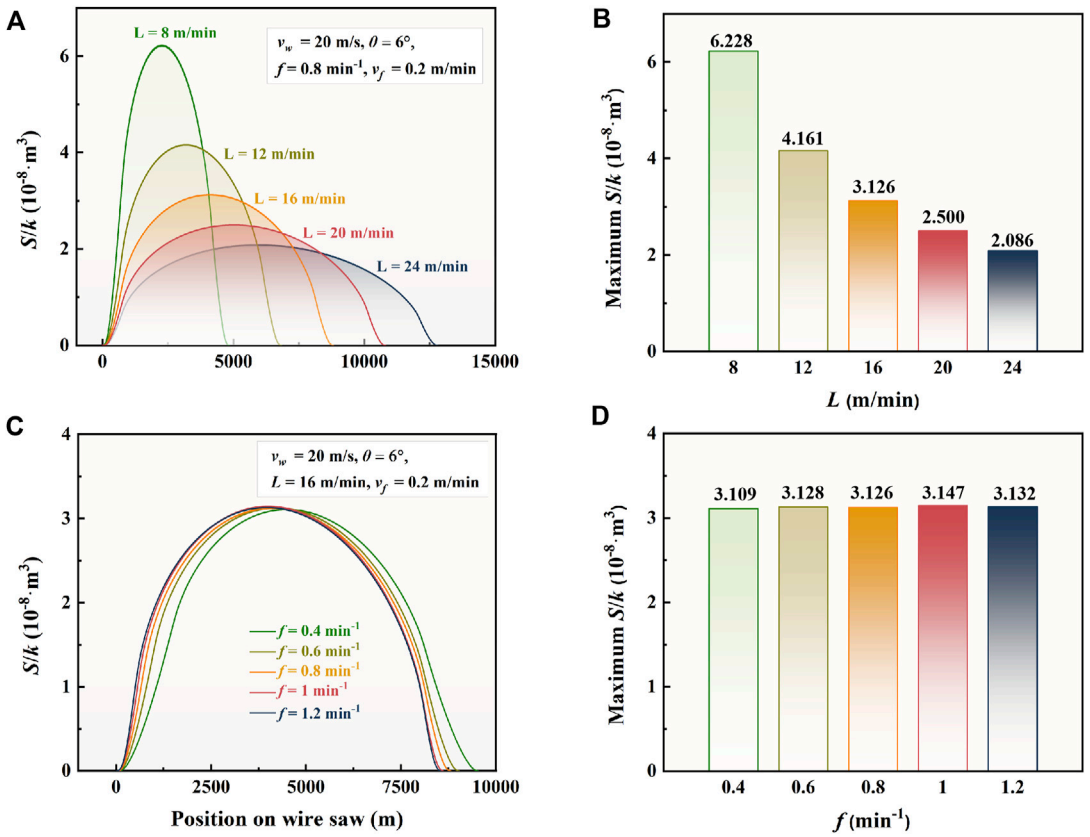

FIGURE 11
Variation of the wear amount of the wire saw for circular workpieces under different setting out lengths **(A,B)** and reciprocating frequencies **(C,D)**.

Step 6: According to Section 2.3, the model of the wire saw for cutting the single piece is established. According to the number of workpieces to be cut, the superimposed matrix is calculated to obtain the wire saw wear model for cutting multiple wafers $multiS_{location}$.

4 Numerical simulation results and discussion

4.1 Numerical simulation of rectangular workpiece

Only the line speed changes, it will not affect the change of the sawing area per cycle, nor the time length of the cycle. The change will only affect the values of t_b and t_f in the cycle, and according to Eq. (1), the speed becomes larger, and the $(t_f + t_b)$ in Eq. (1) becomes smaller, thereby reducing the effect of speed change on the wear of the wire saw.

The feed speed of the workpiece and the length of the wire saw had an obvious impact on the maximum wear of the wire saw, and the maximum rocking angle, wire speed, and reciprocating times have no obvious effect on the maximum wear of the wire saw. The wire saw wear curve of a rectangular workpiece has a stable interval at the middle position, and it presents a changing state at the beginning and end of the curve. Changes in setting out length per minute and workpiece feed speed will lead to increased wire usage during processing. When the length of the wire involved in processing increases, the total volume of workpiece removed does not change, so the volume of workpiece removed evenly on each line will decrease, resulting in reduced wire saw wear as shown inFigure 9A,10C.

4.2 Numerical simulation of circular workpieces

Wire saw wear curve for round workpieces varies throughout the phases. The biggest difference between a round workpiece and a rectangular workpiece is that the sawing area changes during the wire sawing process has a large unevenness.

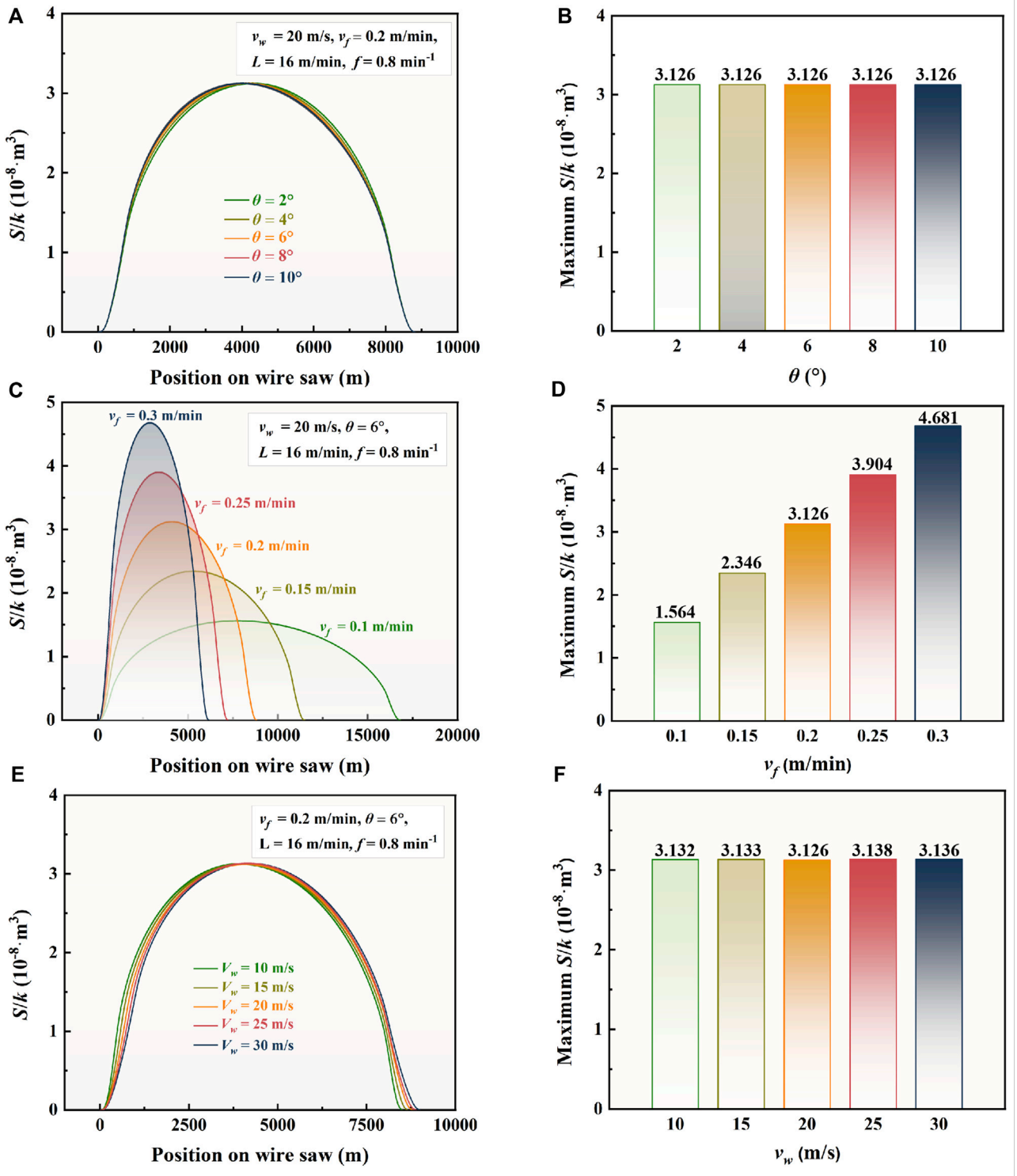

FIGURE 12
Variation of the wear amount of the wire saw for circular workpieces under different maximum rocking angles **(A,B)**, workpiece feed speeds **(C,D)**, and maximum wire speeds **(E,F)**.

During the sawing process, the contact length of the wire saw to the workpiece is the main reason for the unevenness. And this leads to a difference in the wear of the wire saw in the length when sawing round workpieces and rectangular workpieces. However, the situation of wire saw wear under different processing parameters

is similar to that of the rectangular workpiece in Figures 11,12.

5 Conclusion

In this work, the wire saw wear model for multi-wire saw cutting of wafers was built, and the influence of cutting parameters on wear of the diamond wire saw was analyzed through multiple groups of single-factor simulations based on the wear model. From these simulation results and discussions, the conclusions can be summarized as:

1 When the relevant parameters are changed at the same rate, the feed speed of the workpiece and the length of the wire saw had an obvious effect on the maximum wear of the wire saw.
2 The maximum rocking angle, wire speed, and reciprocating times have no obvious effect on the maximum wear of the wire saw.
3 The shape of the workpiece has a significant effect on the wear of the diamond wire saw: the wear on the diamond wire saw was always uneven during cutting the circle ingot, while most of the wear on the diamond wire saw was even during cutting a rectangular ingot.

Data availability statement

The original contributions presented in the study are included in the article/supplementary material, further inquiries can be directed to the corresponding author.

Author contributions

ZY: investigation, data curation, visualization; HH: conceptualization, resources, and writing—review and editing; XL: writing—origianl draft, writing–review and editing.

Acknowledgments

The authors would like to acknowledge the financial supports from the Program for Innovative Research Team at University of the Ministry of Education of China (IRT_17R41), the Natural Science Foundation of Fujian Province (2022J05059), and the Scientific Research Funds of Huaqiao University (605-50Y21024).

Conflict of interest

The authors declare that the research was conducted in the absence of any commercial or financial relationships that could be construed as a potential conflict of interest.

Publisher's note

All claims expressed in this article are solely those of the authors and do not necessarily represent those of their affiliated organizations, or those of the publisher, the editors, and the reviewers. Any product that may be evaluated in this article, or claim that may be made by its manufacturer, is not guaranteed or endorsed by the publisher.

References

Chen, K., Zha, J., Hu, F., Ye, X., Zou, S., Vähänissi, V., et al. (2019). MACE nano-texture process applicable for both single- and multi-crystalline diamond-wire sawn Si solar cells. *Sol. Energy Mat. Sol. Cells* 191, 1–8. doi:10.1016/J.SOLMAT.2018.10.015

Gao, Y., Ge, P., and Liu, T. (2016). Experiment study on electroplated diamond wire saw slicing single-crystal silicon. *Mat. Sci. Semicond. process.* 56, 106–114. doi:10.1016/j.mssp.2016.08.003

Huang, H., Zheng, S. L., and Xu, X. P. (2016). Theoretical research on contact length in the rocking motion wire saw. *Adv. Mat. Res.* 1136, 343–349. doi:10.4028/www.scientific.net/amr.1136.343

Kim, D., Kim, H., Lee, S., and Jeong, H. (2015). Effect of initial deflection of diamond wire on thickness variation of sapphire wafer in multi-wire saw. *Int. J. Precis. Eng. Manuf. -Green. Tech.* 2, 117–121. doi:10.1007/s40684-015-0015-x

Kim, H., Kim, D., Kim, C., and Jeong, H. (2013). Multi-wire sawing of sapphire crystals with reciprocating motion of electroplated diamond wires. *CIRP Ann.* 62, 335–338. doi:10.1016/j.cirp.2013.03.122

Knoblauch, R., Boing, D., Weingaertner, W. L., Wegener, K., Kuster, F., and Xavier, F. A. (2018). Investigation of the progressive wear of individual diamond grains in wire used to cut monocrystalline silicon. *Wear* 414–415, 50–58. doi:10.1016/j.wear.2018.07.025

Kumar, A., Kaminski, S., Melkote, S. N., and Arcona, C. (2016). Effect of wear of diamond wire on surface morphology, roughness and subsurface damage of silicon wafers. *Wear* 365, 163–168. doi:10.1016/j.wear.2016.07.009

Lee, S., Kim, H., Kim, D., and Park, C. (2016). Investigation on diamond wire break-in and its effects on cutting performance in multi-wire sawing. *Int. J. Adv. Manuf. Technol.* 87, 1–8. doi:10.1007/s00170-015-7984-3

Li, Z., Wang, M. J., Pan, X., and Ni, Y. M. (2015). Slicing parameters optimizing and experiments based on constant wire wear loss model in multi-wire saw. *Int. J. Adv. Manuf. Technol.* 81, 329–334. doi:10.1007/s00170-015-7229-5

Liu, Y., and Zhu, Z. (2022). Experimental investigation on diamond wire sawing of Si3N4 ceramics considering the evolution of wire cutting performance. *Ceram. Int.* 48, 17335–17342. doi:10.1016/j.ceramint.2022.02.296

Maeda, H., Takanabe, R., Takeda, A., Matsuda, S., and Kato, T. (2014). High-speed slicing of SiC ingot by high-speed multi-wire saw. *Mat. Sci. Forum* 778–780, 771–775. doi:10.4028/www.scientific.net/msf.778-780.771

Pala, U., Süssmaier, S., Kuster, F., and Wegener, K. (2018). Experimental investigation of tool wear in electroplated diamond wire sawing of silicon. *Procedia CIRP* 77, 371–374. doi:10.1016/j.procir.2018.09.038

Sekhar, H., Fukuda, T., Tanahashi, K., Takato, H., Ono, H., Sampei, Y., et al. (2020). Mechanical strength problem of thin silicon wafers (120 and 140 μm) cut with thinner diamond wires (Si kerf 120 → 100 μm) for photovoltaic use. *Mat. Sci. Semicond. process.* 119, 105209. doi:10.1016/j.mssp.2020.105209

Wang, P., Ge, P., Gao, Y., and Bi, W. (2017). Prediction of sawing force for single-crystal silicon carbide with fixed abrasive diamond wire saw. *Mat. Sci. Semicond. process.* 63, 25–32. doi:10.1016/j.mssp.2017.01.014

Yin, Y., Gao, Y., and Yang, C. (2021). Sawing characteristics of diamond wire cutting sapphire crystal based on tool life cycle. *Ceram. Int.* 47, 26627–26634. doi:10.1016/j.ceramint.2021.06.070

Zhao, Y., Bi, W., and Ge, P. (2021). An on-line inspection method for abrasive distribution uniformity of electroplated diamond wire saw. *J. Manuf. Process.* 71, 290–297. doi:10.1016/j.jmapro.2021.09.041